© 2019. Published by The Company of Biologists Ltd | Development (2019) 146, dev177410. doi:10.1242/dev.177410

RESEARCH REPORT

A homolog of the ALOG family controls corolla tube differentiation in *Torenia fournieri*

Wei Xiao[1,‡,*], Shihao Su[2,‡,§], Tetsuya Higashiyama[2,3] and Da Luo[4]

ABSTRACT

Flowers of honey plants (*Torenia*) face various abiotic stressors, including rain, that can damage pollens and dilute nectar. Many *Torenia* species are thought to have evolved a modified corolla base termed the corolla neck to prevent raindrops from contacting the nectar. Although this hypothesis was postulated long ago, direct validation is lacking. Here, we have evaluated *Torenia fournieri*, the corolla tube of which differentiates into distinct regions: a conical tube above that connects to an inflated base through a constriction. This constriction and inflated base are collectively referred to as the corolla neck. Using transcriptomic sequencing and genome-editing approaches, we have characterized an *ALOG* gene, *TfALOG3*, that is involved in formation of the corolla neck. *TfALOG3* was found expressed in the epidermis of the corolla neck. Cells in the corolla bottom differentiated and expanded in wild-type *T. fournieri*, whereas such cells in *TfALOG3* loss-of-function mutants failed to develop into a corolla neck. Water easily contacted the nectary in the absence of the corolla neck. Taken together, our study unveils a novel gene that controls corolla tube differentiation and demonstrates a hypothetical property of the corolla neck.

KEY WORDS: ALOG, Corolla neck, Corolla tube differentiation, Lamiales, Rain, *Torenia fournieri*

INTRODUCTION

Many nectar-feeding animals prefer high-quality nectar, and plants have evolved multiple ways to protect their nectar reward (Heyneman, 1983; Nachev et al., 2017; Sprengel, 1793). One major threat to nectar is rain, as raindrops can physically injure the corolla, wash away pollen grains, and spoil and dilute nectar (Darwin, 1876; Hagerup, 1950; Sprengel, 1793). Plants that can protect against the damage caused by rain are favored. In 1793, Sprengel described several structures that protect flowers from rain (Sprengel, 1793). Since then, many biologists have recognized floral features that can adapt to bad weather, including an ability to decrease the openness of the flower (Darwin, 1876), a hydrophobic corolla that gathers water at the base (Hagerup, 1950), changes in the flower orientation (Bynum and Smith, 2001; Huang et al., 2002; Tadey and Aizen, 2001) and production of water-resistant pollen (Mao and Huang, 2009).

Many *Torenia* flowers have a corolla neck, which is an enlarged cylindrical structure surrounding the nectary located at the floral base. The corollas of *Torenia* species have differentiated into three regions: a petal lobe, in which petals are separated and exhibit strong zygomorphy; a conical tube, in which different petals fuse together; and a cylindrical corolla neck connected to a conical tube through a constricted region (Fig. S1). The neighboring corolla tissues showed distinct cellular activities according to comparisons of RNA-sequencing data from the conical tubes and corolla necks of *T. fournieri*. We focused on an *ALOG* (*Arabidopsis LSH1* and *Oryza G1*) gene, *TfALOG3*, that is specifically expressed in the corolla neck, indicating its possible role in the development of the corolla neck. We further analyzed the function of *TfALOG3* by generating *TfALOG3* loss-of-function mutants. The corolla neck structure was no longer apparent in the mutant compared with the wild-type flowers. We also observed that water can easily contact the nectary of the mutant flowers, supporting this hypothetical property of the corolla neck in *T. fournieri*.

RESULTS AND DISCUSSION

Corolla necks are present on the flowers of several *Torenia* species

We investigated the flowers of four *Torenia* species: *T. fournieri*, *T. concolor*, *T. violacea* and *T. hybrida*. Except for *T. hybrida*, which is an interspecific hybrid of *T. fournieri* and *T. concolor*, the remaining three species are distributed mostly in tropical and/or subtropical areas, such as East and Southeast Asia, where rainfall is always abundant during the flowering season (eFloras, www.efloras.org/). We observed that all of these species possess a corolla neck at the base of the corolla, where the nectary and nectar are protected (Fig. S1).

To validate the water-repellent property of the corolla neck, we mimicked raindrops by applying different amounts of water containing 0.1% Safranin O dye as an indicator into the corolla tubes of *T. fournieri*. The water ran down to the center of the corolla and stopped once reaching the constricted region (Fig. 1A). Even after increasing the amount of water, water still could not access the nectary (Fig. 1A). Similar results were obtained when we applied 200 µl colored water to the flowers of either *T. concolor* or *T. hybrida* (Fig. S2A). When the water volume reached 400 µl, it forced the flowers to change direction, making the water itself flow out from the drooping flowers (Fig. 1A). These results support the property of the corolla neck hypothesized by Sprengel, at least among *Torenia*.

As biological function relies largely on structural properties, we carefully observed the development of the corolla neck. In a

[1]State Key Laboratory of Biocontrol and Guangdong Key Laboratory of Plant Resources, School of Life Sciences, Sun Yat-sen University, Guangzhou, 510275, China. [2]Institute of Transformative Bio-Molecules (WPI-ITbM), Nagoya University, Furo-cho, Chikusa-ku, Nagoya, Aichi, 464-8601, Japan. [3]Division of Biological Science, Graduate School of Science, Nagoya University, Furo-cho, Chikusa-ku, Nagoya, Aichi, 464-8602, Japan. [4]Key Laboratory of Soybean Molecular Design Breeding, Northeast Institute of Geography and Agroecology, Chinese Academy of Sciences, Changchun, 130102, China.
*Present address: ZMBP-Center for Plant Molecular Biology, University of Tübingen, Auf der Morgenstelle 32, D-72076 Tübingen, Germany.
‡These authors contributed equally to this work

§Author for correspondence (sushihao@itbm.nagoya-u.ac.jp)

S.S., 0000-0002-1953-0242

Received 25 February 2019; Accepted 23 July 2019

Development (2019) 146, dev177410. doi:10.1242/dev.177410

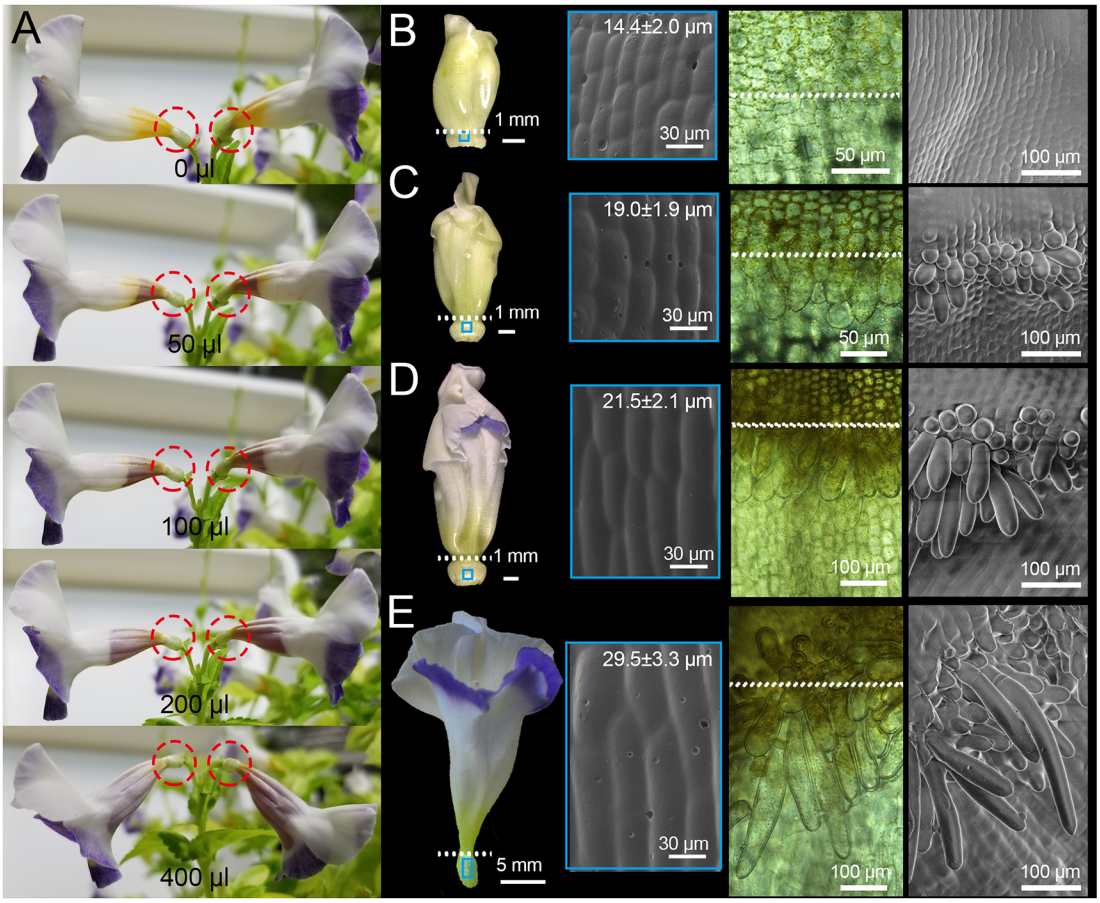

Fig. 1. Function and development of the corolla neck in *Torenia fournieri*. (A) Application of water containing 0.1% Safranin O to flowers. The volumes of water are shown; the red circles indicate the corolla neck. (B-E) Differentiation of the corolla neck in flowers from stages 10 to 13. Each panel shows the intact flower, a scanning electron microscopy image of the outer epidermis (average epidermal cell width is also shown above, *n*=20), a light microscopy image of the developing hairs, and a scanning electron microscopy image of the developing hairs. The blue boxes mark the outer corolla neck epidermis and the white dotted lines indicate the constricted region between the conical tube and corolla neck.

previous study, we divided the process of flower development in *T. fournieri* into 13 stages (Su et al., 2017). The corolla neck became distinguishable at stage 10 and grew rapidly until stage 13 (Fig. 1). Cell expansion was evident when we examined the outer epidermal cells of the corolla neck (Fig. 1). A large amount of yellow pigment accumulated in the inner epidermal cells of the corolla bottom beginning at stage 10 (Fig. 1B). Cells from the constricted region began to differentiate (Fig. 1C) and further developed into a row of hair cells (Fig. 1D,E). We also examined the corresponding regions in *T. concolor* or *T. hybrida*. To our surprise, no hair cells existed in the constricted region of *T. concolor*, and short hair cells developed in the interspecific hybrid *T. hybrida* (Fig. S2C).

To test whether the hair cells on the corolla neck also functioned to prevent rain from entering, we removed the reproductive organs and dissected the corolla tubes. By directly applying 20 µl colored water into the cut corolla bottoms, the water traveled to the bottom of the *T. concolor* corolla but was blocked in the constricted region of *T. hybrida* (Fig. S2C). These results indicate that, although the constricted region together with the pistil is sufficient to prevent water access, hairs on the constricted region may decrease the ability of water to penetrate. Because under natural conditions, rain is associated mostly with wind (which makes the rain easier to enter the flower), the presentation of hairs functions as another mechanism with which to restrict water access. Compared with *T. fournieri*, which grows erect, *T. concolor* has a decumbent growth habit, making its flowers approach the ground; in this case, the wind may not be a problem.

The conical tube and the corolla neck have distinct cellular activities

We performed transcriptome sequencing to identify the potential factors involved in regulation of the corolla neck (Fig. 2). Hormone signal transduction and DNA replication were the most enriched pathways among the genes expressed in the corolla neck; however, the biosynthesis of secondary metabolites and flavonoid biosynthesis were the most enriched pathways among the genes expressed in the conical tube, supporting their distinct cellular activities (Fig. 2A,B). These two tissues displayed different expression profiles: 2550 and 1806 genes were more highly expressed in the corolla neck and conical tube, respectively (Fig. 2C). Next, we focused on the genes encoding transcription factors that were more highly expressed in the corolla neck.

The top 10 differentially expressed transcription factor genes included one *ALOG*, one *KNAT6*-like *KNOX*, one *AP2*, one *MYB*, several *AGAMOUS*-like *MADS* and *YABBY* genes (Fig. 2D). Phylogenetic analyses of these 10 candidate genes were carried out (Fig. S3). Four *MADS* genes belonged to AGAMOUS-clade factors, and previous studies have reported that these genes are highly expressed in stamens as well as in pistils (Fig. S3B) and may play a role in the development of plant reproductive organs

Development (2019) 146, dev177410. doi:10.1242/dev.177410

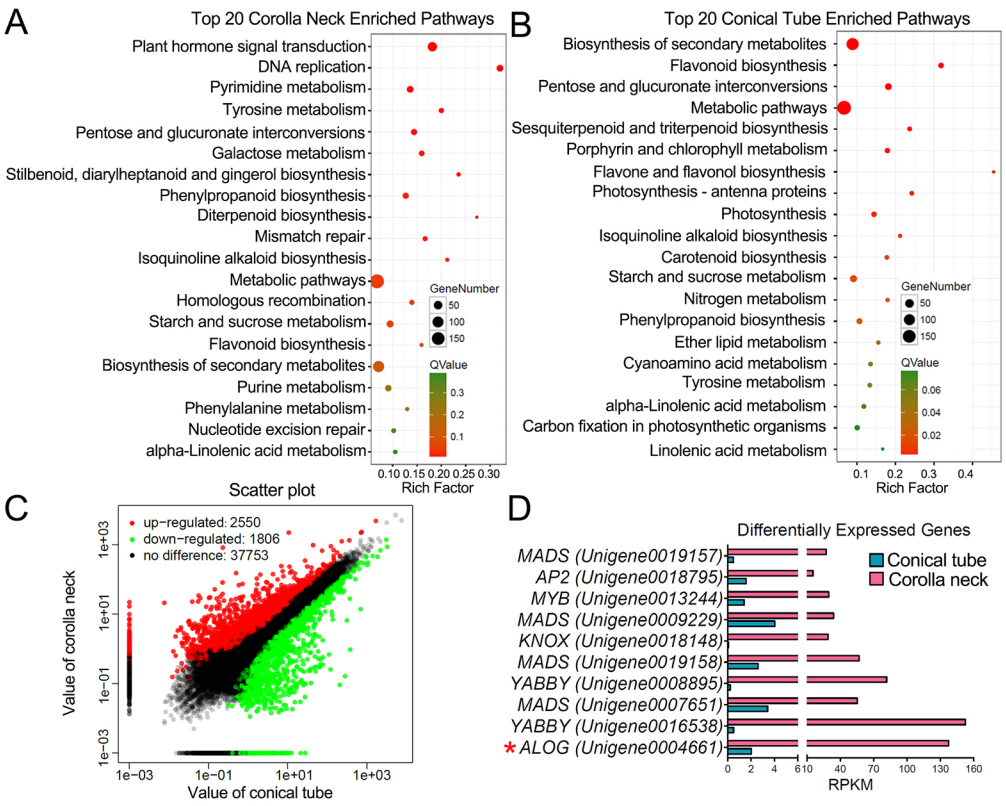

Fig. 2. Differentially expressed genes between two regions of the corolla tube. (A) The top 20 pathways enriched among genes expressed in the corolla neck. (B) The top 20 pathways enriched among genes expressed in the conical tube. (C) The scatterplot illustrates differentially expressed genes between the corolla neck and conical tube. (D) The top 10 most highly expressed transcription factors in the corolla neck. The reads per kilobase per million mapped reads value for each unigene is shown; the red asterisk marks the candidate gene evaluated.

(Nishijima et al., 2016; Su et al., 2018b). Two *YABBY*-like genes are the homologs of *Arabidopsis CRC* (Fig. S3C), which is required for floral stem cell maintenance and carpel development (Bowman and Smyth, 1999; Yamaguchi et al., 2017). The *KNOX*-like candidate was homologous to *Arabidopsis KNAT2* and *KNAT6* (Fig. S3D), two genes enriched in the shoot apical meristem (SAM) and organ boundaries, which are important for the maintenance of SAM and organ separation (Belles-Boix et al., 2006). The *MYB*-like gene shows homology to *Arabidopsis ATMYB16* and *ATMYB106* (Fig. S3E), which are involved in the differentiation of the petal epidermis and cutin formation (Baumann et al., 2007; Kannangara et al., 2007; Oshima et al., 2013). The *AP2*-like gene shares homology to *Arabidopsis APETALA2* (Fig. S3F), which is expressed in the floral meristem and various floral organs, and regulates floral stem cells and organ differentiation (Bowman et al., 1991; Drews et al., 1991; Krogan et al., 2012; Wollmann et al., 2010). Among the 10 genes, we selected the *ALOG* gene (*Unigene0004661*) as our candidate, due to a lack of sufficient functional information about this gene family. To date, several members from the ALOG family have been functionally elucidated, suggesting their various roles in plant development (Cho and Zambryski, 2011; Lei et al., 2019; MacAlister et al., 2012; Takeda et al., 2011; Yoshida et al., 2013, 2009).

TfALOG3 is a candidate gene involved in corolla neck differentiation

Seven *ALOG* genes have been isolated previously from *T. fournieri*, and we confirmed the identification of *Unigene0004661* as *TfALOG3* after comparison with published sequences (Fig. S3A). The gene is expressed mainly in flower buds, and it encodes a nuclear localized protein belonging to the euALOG1 subclade of ALOG proteins (Xiao et al., 2018). We examined the expression of *TfALOG3*, together with that of paralog *TfALOG1*, by reverse-transcription (RT)-PCR (Fig. 3A,B). *TfALOG1* was expressed in both the conical tube and corolla neck, whereas *TfALOG3* was expressed specifically in the corolla neck, suggesting functional diversification of these two paralogs (Fig. 3B). As mentioned before, *T. concolor* is devoid of hairs in the constricted region; thus, we measured *TfALOG3* homolog expression in dissected *T. concolor* corollas (Fig. S4). Similar to *T. fournieri*, *TcALOG3* was also expressed specifically in the corolla neck, indicating that ALOG3 is likely to be involved in the 3D shaping of the neck, rather than in the specification of the hair cell fate.

We further determined the spatiotemporal expression pattern of *TfALOG3* by RNA *in situ* hybridization. During the early phase (stage 6), *TfALOG3* was expressed at the bottom of the corolla, where petal and stamen whorls fuse together (Fig. 3C). No specific signal was detected from the negative control sense probe (Fig. 3E). During the late phase (stages 9 and 10), *TfALOG3* was expressed specifically in the entire corolla neck, with the strongest expression in the inner and outer epidermis (Fig. 3D,F,G), and no expression in the nectar region (Fig. 3D). The specific expression of *TfALOG3* strongly supports its potential function in differentiation of the corolla neck.

Functional analysis of *TfALOG3*

To elucidate the function of *TfALOG3*, we generated loss-of-function mutants using the CRISPR/Cas9 genome editing method. Two different plasmids coding for two and three guide RNAs, respectively, were constructed (Fig. S5A). We performed transformation using two *T. fournieri* cultivars with different floral colors. Mutations were detected in three independent transgenic lines, leading to frame shifts and premature termination (Fig. S5B). In the first mutant, single nucleotide insertions were observed in both targeted sites; in the second mutant, only one nucleotide insertion was detected in the first targeted site (Fig. S5B).

Development (2019) 146, dev177410. doi:10.1242/dev.177410

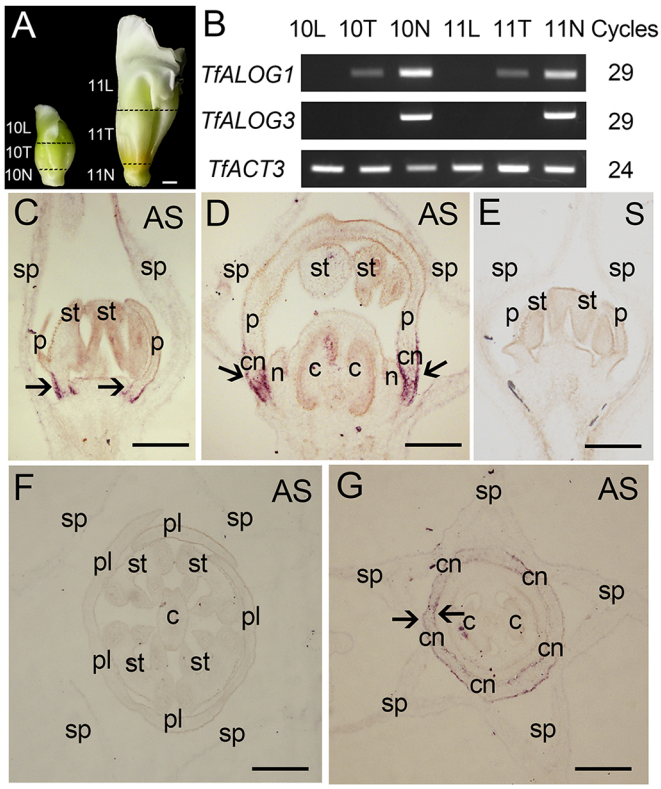

Fig. 3. Expression pattern of the candidate *ALOG* gene *TfALOG3*. (A) The materials used in this assay. Scale bar: 1 mm. (B) Reverse-transcription PCR analysis of *TfALOG1*/*3*. Gene names and number of PCR cycles are shown on the left and right sides of each panel, respectively. β-Actin (*TfACT3*) expression was measured as an internal control. 10, stage 10 floral bud; 11, stage 11 floral bud; L, petal lobe; T, conical tube; N, corolla neck. (C-G) RNA *in situ* hybridization of *TfALOG3* in different flower buds. Longitudinal sections of stage 6 (C,E) and stage 9 (D) floral buds, and transverse sections of a stage 10 floral bud (F,G). AS, antisense probe; S, control sense probe; sp, sepal; p, petal; st, stamen; c, carpel; pl, petal lobe; n, nectar; cn, corolla neck. Arrows indicate the sites of *TfALOG3* mRNA expression. Scale bars: 100 µm.

In the third mutant, single nucleotide insertions were found in the first and third targeted sites, together with a single nucleotide substitution in the second targeted site (Fig. S5B).

Comparing the floral morphologies between the wild-type and mutant plants, we found that the corolla neck had disappeared in the mutant flowers (Fig. 4A-C, Fig. S6A,B, Fig. S7). Yellow pigmentation was observed at the base of the conical tube in the wild-type flowers, whereas the enlarged corolla neck was whiter (Fig. 4A, Fig. S6A). However, the bottom of the corolla was pigmented in the mutant flowers, and the enlarged corolla neck failed to differentiate (Fig. 4A-C, Fig. S6A,B). Both the inner and outer epidermal cells were smaller in the mutant compared with wild-type plants (Fig. 4D). A row of hairs was present in the boundary between the conical tube and corolla neck in the wild-type flowers, but was no longer apparent in the mutant flowers (Fig. S8). Thus, we concluded that TfALOG3 is involved in regulation of corolla neck development.

During the late stages of petal developmental, cells increase in volume via vacuolation (Huang and Irish, 2016; Sugimoto-Shirasu and Roberts, 2003). In *Arabidopsis*, the gene encoding the basic helix-loop-helix transcription factor BIGPETALp (BPEp) is regulated by jasmonate signaling (Brioudes et al., 2009). By interacting with AUXIN RESPONSE FACTOR 8, BPEp limits cell expansion and thus regulates petal growth (Szécsi et al., 2006; Varaud et al., 2011). As ARFs function redundantly during multiple aspects of organ development, other ARFs may also be involved in petal morphogenesis. Our transcriptomic analyses indicated high enrichment of factors involved in hormone signal transduction as well as seven *ARF* unigenes in the corolla neck (Fig. 2A, Fig. S9A). After examining the expression of these genes in the wild-type and mutant plants, significant downregulation in the mutant corolla of an *ARF4*-like gene was detected, suggesting that this gene is a potential downstream target of TfALOG3 in the regulation of corolla neck development (Fig. S9B-E).

As the cylindrical corolla neck prevents water from entering the nectary, we performed similar assays using the wild-type and mutant flowers. When applying 200 µl colored water to the flowers, we found that the water easily entered the nectary of the mutant flower compared with the wild-type flower (Fig. 4E, Fig. S6C,D). To exclude the effects of male or female reproductive organs, we dissected the corolla bottoms from the flowers and positioned them on slides. After pipetting 20 µl colored water into the cut corollas, we observed that the water was blocked in the neck region of the wild-type corolla, whereas it ran to the bottom of the mutant corolla (Fig. 4F,G). These results indicate the indispensability of the corolla neck. Based on these observations, we propose a potential model to explain how the corolla neck prevents raindrops from entering the flower (Fig. S10). In *T. fournieri*, the pistil and constriction at the top of the corolla neck, together with hairs, form an intact 'cover'. When raindrops enter the corolla, they are restricted to this region, thus preventing dilution of the nectar in the nectar container (Fig. S10). However, in the mutant plants, the corolla and pistil fail to form a 'cover', allowing the raindrops to enter the nectar container and spoil the nectar (Fig. S10).

Possible functions of the corolla neck

The flowers of *T. fournieri* are upward facing and have relatively wide openings. Raindrops readily enter the flower and gravitate towards its nectar. Thus, the nectar must be secured by measures such as development of a corolla neck. In the future, side-by-side comparisons of pollinator visits between wild-type and mutant flowers would provide a clearer demonstration of the ecological function. Moreover, the corolla neck may also be involved in other biological processes such as maintenance of the nectar microclimate or protection from nectar robbers. For example, many downward-facing flowers of the *Penstemon* and *Salvia* genera also have corolla neck-like structures. In these species, the corolla neck may serve as mechanical protection from nectar robbers. These functions need further exploration. As the origin of this corolla structure may be a key innovation during evolutionary history, it will be an interesting issue in the future to explore how the corolla structure originated.

A novel gene controlling differentiation of the corolla tube

The ABC model explains how the concentric whorls of floral organs are genetically specified, and numerous studies support that B class genes play important roles in the development of petals and stamens (Coen and Meyerowitz, 1991; Irish, 2017). In *T. fournieri*, two B class factors, TfDEF and TfGLO, have been characterized (Sasaki et al., 2014). In *TfDEF*/*TfGLO*-ox plants, sepals change to petal-like structures; however, the petaloid sepals lack a corolla neck at the bottom (Sasaki et al., 2014). When *TfDEF* and *TfGLO* are co-suppressed, the petals exhibit sepaloid organs without affecting formation of the corolla neck, indicating that the corolla neck is a B-gene-independent floral structure (Sasaki et al., 2010, 2014).

Development (2019) 146, dev177410. doi:10.1242/dev.177410

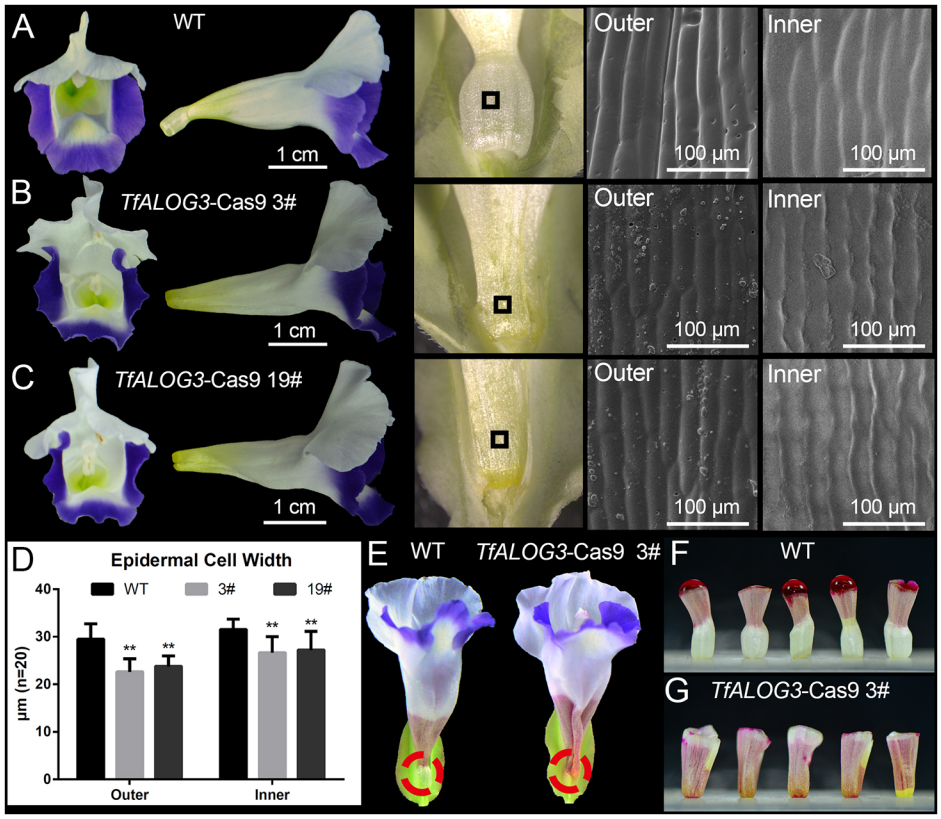

Fig. 4. Functional analysis of TfALOG3. (A-C) Front, side and zoomed-in views of *Torenia fournieri* wild-type (A) and two independent *TfALOG3*-Cas9 flower lines: 3# (B) and 19# (C). Scanning electron microscopy images of outer and inner epidermal cells from each flower, marked by a black box, are also shown. (D) Statistical comparison of epidermal cell width. The two asterisks indicate significant differences between the mutant and wild-type plants (P<0.01). (E) Application of 200 µl water containing 0.1% Safranin O to two flowers. The red dashed circle indicates the corolla neck. (F,G). Application of 20 µl water containing 0.1% Safranin O to different cut corolla bottoms.

To summarize, our study revealed two distinct regions in the corolla bottom and characterized an *ALOG* gene involved in genetic regulation in the corolla neck. In the future, it would be worthwhile to explore the underlying molecular mechanisms controlling differentiation of the corolla tube using *T. fournieri* as a new eco-evo-devo model.

MATERIALS AND METHODS

Plant materials

Torenia spp. plants were cultured at 25°C under a 16 h:8 h light: dark cycle. To produce sterile plants, *T. fournieri* seeds were sterilized by a series of washes with ethanol, sterile water and then 10% sodium hypochlorite, with four rinses in sterile water. The sterile seeds were germinated on half-strength MS culture medium and refreshed with new medium every 4 weeks.

Microcopy

To observe epidermal cells, floral buds of different stages were collected and dissected under a stereomicroscope. Three types of impression materials were used to produce the epoxy replica, as described previously (Su et al., 2018a). The replicas were sputtered with gold and examined under a JEOL JSM 6360LV scanning electron microscope. To calculate the epidermal cell width, 20 randomly selected cells were measured using Adobe Photoshop CS6 and statistical calculations were performed using multiple *t*-tests. To observe hair cell development, corollas of different stages were dissected on slides and mounted with mounting medium. To avoid possible dehydration, the slides were immediately examined under a Zeiss Axio Imager light microscope.

Transcriptomic sequencing and analyzing

We sequenced the transcriptome of the conical tube and corolla neck in two biological replicates. Stage 11 corolla tubes were collected and dissected into two regions, including the conical petal tube and corolla neck. Total RNA was extracted using the Plant RNA Kit (Omega Bio-Tek). Poly(A) mRNA was purified and fragmented prior to sequencing. First-strand cDNA was synthesized using a random hexamer primer, followed by second-strand cDNA synthesis. The sequencing adaptors were ligated to the fragments, which were purified by electrophoresis and amplified by PCR as described previously (Su et al., 2018a). The libraries were paired-end sequenced on the Illumina HiSeq 2000 platform and ∼6 Gb (35.5-43.5 million sequencing reads) were obtained. After obtaining the clean reads, two rounds of *de novo* assembly were carried out using the Trinity (containing Inchworm, Chrysalis and Butterfly) and CAP3 programs (Gene Denovo Biotechnology) (Haas et al., 2013; Huang and Madan, 1999). After assembly, 42,756 unigenes were obtained, with N50=1901 bp. The reads per kilobase per million mapped reads values were calculated to determine the relative expression of each unigene, and gene ontology annotations were determined by the Blast2GO program (Conesa et al., 2005; Mortazavi et al., 2008). Differentially expressed genes were identified as those with a fold change ≥2 and a false discovery rate <0.05 using the edgeR package (www.r-project.org/). To determine differentially expressed transcription factor genes, we applied ‘log2 Ratio (WT-12-down/WT-12-up) ≥3’ and ‘WT-12-down_count for descending order’ rules. Differentially expressed unigenes and top 10 differentially expressed transcription factor genes are listed in Table S2.

Expression analysis

Total RNA was extracted from different tissues using the Plant RNA Kit (Omega Bio-Tek). For RT-PCR analysis, the cDNA templates were prepared using the RevertAid First Strand cDNA Synthesis Kit (Thermo Fisher Scientific). For quantitative RT-PCR, the cDNA templates were prepared using the PrimeScript RT reagent Kit with the gDNA Eraser (Takara). PCR was performed using the LightCycler 480 Real-Time PCR System (Roche) according to the manual. β-Actin (*TfACT3*) expression was measured as an internal control. The primers used in this study are listed in Table S1.

Inflorescences or floral buds were fixed in FAA (formalin-acetic acid-alcohol) fixative containing 50% (v/v) ethanol, 3.7% (v/v) formaldehyde and 5% (v/v) acetic acid for RNA *in situ* hybridization. The tissues were

embedded with Paraplast (Sigma-Aldrich) after treatment with an ethanol series and xylene solution. The probes were labeled with digoxigenin-UTP. Hybridization was performed as described previously (Coen et al., 1990). The primers used in this study are listed in Table S1.

Plant transformation

The CRISPR/Cas9 binary vector (provided by Prof. Yaoguang Liu, South China Agricultural University, China) was constructed according to Ma et al. (2015). Target sequences with a protospacer adjacent motif (NGG) are shown in Fig. S5A. Transformation of the vector into *T. fournieri* was performed as reported previously (Aida, 2012; Su et al., 2017). The edited *TfALOG3* sequences are shown in Fig. S5B.

Accession numbers

The raw data from the RNA-sequencing analyses have been deposited into SRA under accession numbers SRR8449829, SRR8449830, SRR8449831 and SRR8449832.

Acknowledgements

We thank Prof. Norihiro Ohtsubo from Kyoto Prefectural University (Japan), Prof. Katsutomo Sasaki from National Agriculture and Food Research Organization (Japan) and Miss Naoe Ando from Nagoya University (Japan) for their patient instructions on plant transformation, and Dr Naoki Yanagisawa from Nagoya University (Japan) for his help on scanning electronic microscopy. We appreciate the editor and three anonymous reviewers for their valuable comments on the manuscript. We are also grateful to Dr Wuxiu Guo from Sun Yat-sen University (China) for helpful discussions and to Mr Chao Huang for his help on collecting *T. voilacea* in the field.

Competing interests

The authors declare no competing or financial interests.

Author contributions

Conceptualization: W.X., S.S., T.H., D.L.; Methodology: W.X., S.S.; Validation: S.S.; Formal analysis: W.X., S.S.; Investigation: W.X., S.S.; Data curation: W.X.; Writing - original draft: S.S.; Writing - review & editing: W.X., S.S., T.H., D.L.; Supervision: T.H., D.L.; Funding acquisition: T.H.

Funding

This work is supported by Grants-in-Aid for Scientific Research from the Ministry of Education, Culture, Sports, Science, and Technology of Japan (6H06465 and 16K21727 to T.H.). S.S. is supported by an overseas postdoctoral fellowship from the Japan Society for the Promotion of Science.

Data availability

The raw data from the RNA-sequencing analyses have been deposited into SRA under accession numbers SRR8449829, SRR8449830, SRR8449831 and SRR8449832.

Supplementary information

Supplementary information available online at
http://dev.biologists.org/lookup/doi/10.1242/dev.177410.supplemental

References

Aida, R. (2012). A protocol for transformation of *Torenia*. *Methods Mol. Biol.* **847**, 267-274. doi:10.1007/978-1-61779-558-9_23

Baumann, K., Perez-Rodriguez, M., Bradley, D., Venail, J., Bailey, P., Jin, H., Koes, R., Roberts, K. and Martin, C. (2007). Control of cell and petal morphogenesis by R2R3 MYB transcription factors. *Development* **134**, 1691-1701. doi:10.1242/dev.02836

Belles-Boix, E., Hamant, O., Witiak, S. M., Morin, H., Traas, J. and Pautot, V. (2006). *KNAT6*: an Arabidopsis homeobox gene involved in meristem activity and organ separation. *Plant Cell* **18**, 1900-1907. doi:10.1105/tpc.106.041988

Bowman, J. L. and Smyth, D. R. (1999). *CRABS CLAW*, a gene that regulates carpel and nectary development in Arabidopsis, encodes a novel protein with zinc finger and helix-loop-helix domains. *Development* **126**, 2387-2396.

Bowman, J. L., Smyth, D. R. and Meyerowitz, E. M. (1991). Genetic interactions among floral homeotic genes of Arabidopsis. *Development* **112**, 1-20.

Brioudes, F., Joly, C., Szécsi, J., Varaud, E., Leroux, J., Bellvert, F., Bertrand, C. and Bendahmane, M. (2009). Jasmonate controls late development stages of petal growth in *Arabidopsis thaliana*. *Plant J.* **60**, 1070-1080. doi:10.1111/j.1365-313X.2009.04023.x

Bynum, M. R. and Smith, W. K. (2001). Floral movements in response to thunderstorms improve reproductive effort in the alpine species *Gentiana algida* (Gentianaceae). *Am. J. Bot.* **88**, 1088-1095. doi:10.2307/2657092

Cho, E. and Zambryski, P. C. (2011). Organ boundary1 defines a gene expressed at the junction between the shoot apical meristem and lateral organs. *Proc. Natl. Acad. Sci. USA* **108**, 2154-2159. doi:10.1073/pnas.1018542108

Coen, E. S. and Meyerowitz, E. M. (1991). The war of the whorls: genetic interactions controlling flower development. *Nature* **353**, 31-37. doi:10.1038/353031a0

Coen, E. S., Romero, J. M., Doyle, S., Elliott, R., Murphy, G. and Carpenter, R. (1990). *floricaula*: a homeotic gene required for flower development in *Antirrhinum majus*. *Cell* **63**, 1311-1322. doi:10.1016/0092-8674(90)90426-F

Conesa, A., Gotz, S., Garcia-Gomez, J. M., Terol, J., Talon, M. and Robles, M. (2005). Blast2GO: a universal tool for annotation, visualization and analysis in functional genomics research. *Bioinformatics* **21**, 3674-3676. doi:10.1093/bioinformatics/bti610

Darwin, C. R. (1876). *The Effects of Cross and Self-Fertilisation in the Vegetable Kingdom*. London: John Murray.

Drews, G. N., Bowman, J. L. and Meyerowitz, E. M. (1991). Negative regulation of the Arabidopsis homeotic gene *AGAMOUS* by the *APETALA2* product. *Cell* **65**, 991-1002. doi:10.1016/0092-8674(91)90551-9

Haas, B. J., Papanicolaou, A., Yassour, M., Grabherr, M., Blood, P. D., Bowden, J., Couger, M. B., Eccles, D., Li, B., Lieber, M. et al. (2013). De novo transcript sequence reconstruction from RNA-seq using the Trinity platform for reference generation and analysis. *Nat. Protoc.* **8**, 1494-1512. doi:10.1038/nprot.2013.084

Hagerup, O. (1950). *Rain-Pollination*. E. Munksgaard.

Heyneman, A. J. (1983). Optimal sugar concentrations of floral nectars -dependence on sugar intake efficiency and foraging costs. *Oecologia* **60**, 198-213. doi:10.1007/BF00379522

Huang, T. and Irish, V. F. (2016). Gene networks controlling petal organogenesis. *J. Exp. Bot.* **67**, 61-68. doi:10.1093/jxb/erv444

Huang, X. and Madan, A. (1999). CAP3: A DNA sequence assembly program. *Genome Res.* **9**, 868-877. doi:10.1101/gr.9.9.868

Huang, S.-Q. Takahashi, Y. and Dafni, A. (2002). Why does the flower stalk of *Pulsatilla cernua* (Ranunculaceae) bend during anthesis? *Am. J. Bot.* **89**, 1599-1603. doi:10.3732/ajb.89.10.1599

Irish, V. (2017). The ABC model of floral development. *Curr. Biol.* **27**, R887-R890. doi:10.1016/j.cub.2017.03.045

Kannangara, R., Branigan, C., Liu, Y., Penfield, T., Rao, V., Mouille, G., Hofte, H., Pauly, M., Riechmann, J. L. and Broun, P. (2007). The transcription factor WIN1/SHN1 regulates cutin biosynthesis in *Arabidopsis thaliana*. *Plant Cell* **19**, 1278-1294. doi:10.1105/tpc.106.047076

Krogan, N. T., Hogan, K. and Long, J. A. (2012). APETALA2 negatively regulates multiple floral organ identity genes in Arabidopsis by recruiting the co-repressor TOPLESS and the histone deacetylase HDA19. *Development* **139**, 4180-4190. doi:10.1242/dev.085407

Lei, Y., Su, S., He, L., Hu, X. and Luo, D. (2019). A member of the *ALOG* gene family has a novel role in regulating nodulation in *Lotus japonicus*. *J. Integr. Plant Biol.* **61**, 463-477. doi:10.1111/jipb.12711

Ma, X., Zhang, Q., Zhu, Q., Liu, W., Chen, Y., Qiu, R., Wang, B., Yang, Z., Li, H., Lin, Y. et al. (2015). A robust CRISPR/Cas9 system for convenient, high-efficiency multiplex genome editing in monocot and dicot plants. *Mol. Plant* **8**, 1274-1284. doi:10.1016/j.molp.2015.04.007

MacAlister, C. A., Park, S. J., Jiang, K., Marcel, F., Bendahmane, A., Izkovich, Y., Eshed, Y. and Lippman, Z. B. (2012). Synchronization of the flowering transition by the tomato *TERMINATING FLOWER* gene. *Nat. Genet.* **44**, 1393-1398. doi:10.1038/ng.2465

Mao, Y.-Y. and Huang, S.-Q. (2009). Pollen resistance to water in 80 angiosperm species: flower structures protect rain-susceptible pollen. *New Phytol.* **183**, 892-899. doi:10.1111/j.1469-8137.2009.02925.x

Mortazavi, A., Williams, B. A., McCue, K., Schaeffer, L. and Wold, B. (2008). Mapping and quantifying mammalian transcriptomes by RNA-Seq. *Nat. Methods* **5**, 621-628. doi:10.1038/nmeth.1226

Nachev, V., Stich, K. P., Winter, C., Bond, A., Kamil, A. and Winter, Y. (2017). Cognition-mediated evolution of low-quality floral nectars. *Science* **355**, 75-78. doi:10.1126/science.aah4219

Nishijima, T., Tomoya, N. and Tomoko, N. (2016). A novel “petaloid” mutant of Torenia (*Torenia fournieri* Lind. ex Fourn.) bears double flowers through insertion of the DNA transposon Ttf1 into a C-class floral homeotic gene. *Horticult. J.* **85**, 272-283. doi:10.2503/hortj.MI-108

Oshima, Y., Shikata, M., Koyama, T., Ohtsubo, N., Mitsuda, N. and Ohme-Takagi, M. (2013). MIXTA-like transcription factors and WAX INDUCER1/SHINE1 coordinately regulate cuticle development in Arabidopsis and *Torenia fournieri*. *Plant Cell* **25**, 1609-1624. doi:10.1105/tpc.113.110783

Sasaki, K., Aida, R., Yamaguchi, H., Shikata, M., Niki, T., Nishijima, T. and Ohtsubo, N. (2010). Functional divergence within class B MADS-box genes *TfGLO* and *TfDEF* in *Torenia fournieri* Lind. *Mol. Genet. Genomics* **284**, 399-414. doi:10.1007/s00438-010-0574-z

Sasaki, K., Yamaguchi, H., Nakayama, M., Aida, R. and Ohtsubo, N. (2014). Co-modification of class B genes *TfDEF* and *TfGLO* in *Torenia fournieri* Lind. alters

both flower morphology and inflorescence architecture. *Plant Mol. Biol.* **86**, 319-334. doi:10.1007/s11103-014-0231-8

Sprengel, C. K. (1793). *Das entdeckte Geheimnis der Natur im Bau und in der Befruchtung der Blumen*. Berlin F. Vieweg.

Su, S., Xiao, W., Guo, W., Yao, X., Xiao, J., Ye, Z., Wang, N., Jiao, K., Lei, M., Peng, Q. et al. (2017). The CYCLOIDEA-RADIALIS module regulates petal shape and pigmentation, leading to bilateral corolla symmetry in *Torenia fournieri* (Linderniaceae). *New Phytol.* **215**, 1582-1593. doi:10.1111/nph.14673

Su, S., Shao, X., Zhu, C., Xu, J., Lu, H., Tang, Y., Jiao, K., Guo, W., Xiao, W., Liu, Z. et al. (2018a). Transcriptome-wide analysis reveals the origin of peloria in Chinese Cymbidium (*Cymbidium sinense*). *Plant Cell Physiol.* **59**, 2064-2074. doi:10.1093/pcp/pcy130

Su, S., Shao, X., Zhu, C., Xu, J., Tang, Y., Luo, D. and Huang, X. (2018b). An AGAMOUS-like factor is associated with the origin of two domesticated varieties in *Cymbidium sinense* (Orchidaceae). *Hortic Res.* **5**, 48. doi:10.1038/s41438-018-0052-z

Sugimoto-Shirasu, K. and Roberts, K. (2003). "Big it up": endoreduplication and cell-size control in plants. *Curr. Opin. Plant Biol.* **6**, 544-553. doi:10.1016/j.pbi.2003.09.009

Szécsi, J., Joly, C., Bordji, K., Varaud, E., Cock, J. M., Dumas, C. and Bendahmane, M. (2006). BIGPETALp, a bHLH transcription factor is involved in the control of Arabidopsis petal size. *EMBO J.* **25**, 3912-3920. doi:10.1038/sj.emboj.7601270

Tadey, M. and Aizen, M. A. (2001). Why do flowers of a hummingbird-pollinated mistletoe face down? *Funct. Ecol.* **15**, 782-790. doi:10.1046/j.0269-8463.2001.00580.x

Takeda, S., Hanano, K., Kariya, A., Shimizu, S., Zhao, L., Matsui, M., Tasaka, M. and Aida, M. (2011). CUP-SHAPED COTYLEDON1 transcription factor activates the expression of *LSH4* and *LSH3*, two members of the ALOG gene family, in shoot organ boundary cells. *Plant J.* **66**, 1066-1077. doi:10.1111/j.1365-313X.2011.04571.x

Varaud, E., Brioudes, F., Szécsi, J., Leroux, J., Brown, S., Perrot-Rechenmann, C. and Bendahmane, M. (2011). AUXIN RESPONSE FACTOR8 regulates Arabidopsis petal growth by interacting with the bHLH transcription factor BIGPETALp. *Plant Cell* **23**, 973-983. doi:10.1105/tpc.110.081653

Wollmann, H., Mica, E., Todesco, M., Long, J. A. and Weigel, D. (2010). On reconciling the interactions between APETALA2, miR172 and AGAMOUS with the ABC model of flower development. *Development* **137**, 3633-3642. doi:10.1242/dev.036673

Xiao, W., Ye, Z., Yao, X., He, L., Lei, Y., Luo, D. and Su, S. (2018). Evolution of ALOG gene family suggests various roles in establishing plant architecture of *Torenia fournieri*. *BMC Plant Biol.* **18**, 204. doi:10.1186/s12870-018-1431-1

Yamaguchi, N., Huang, J., Xu, Y., Tanoi, K. and Ito, T. (2017). Fine-tuning of auxin homeostasis governs the transition from floral stem cell maintenance to gynoecium formation. *Nat. Commun.* **8**, 1125. doi:10.1038/s41467-017-01252-6

Yoshida, A., Suzaki, T., Tanaka, W. and Hirano, H.-Y. (2009). The homeotic gene *Long Sterile Lemma* (*G1*) specifies sterile lemma identity in the rice spikelet. *Proc. Natl. Acad. Sci. USA* **106**, 20103-20108. doi:10.1073/pnas.0907896106

Yoshida, A., Sasao, M., Yasuno, N., Takagi, K., Daimon, Y., Chen, R., Yamazaki, R., Tokunaga, H., Kitaguchi, Y., Sato, Y. et al. (2013). TAWAWA1, a regulator of rice inflorescence architecture, functions through the suppression of meristem phase transition. *Proc. Natl. Acad. Sci. USA* **110**, 767-772. doi:10.1073/pnas.1216151110

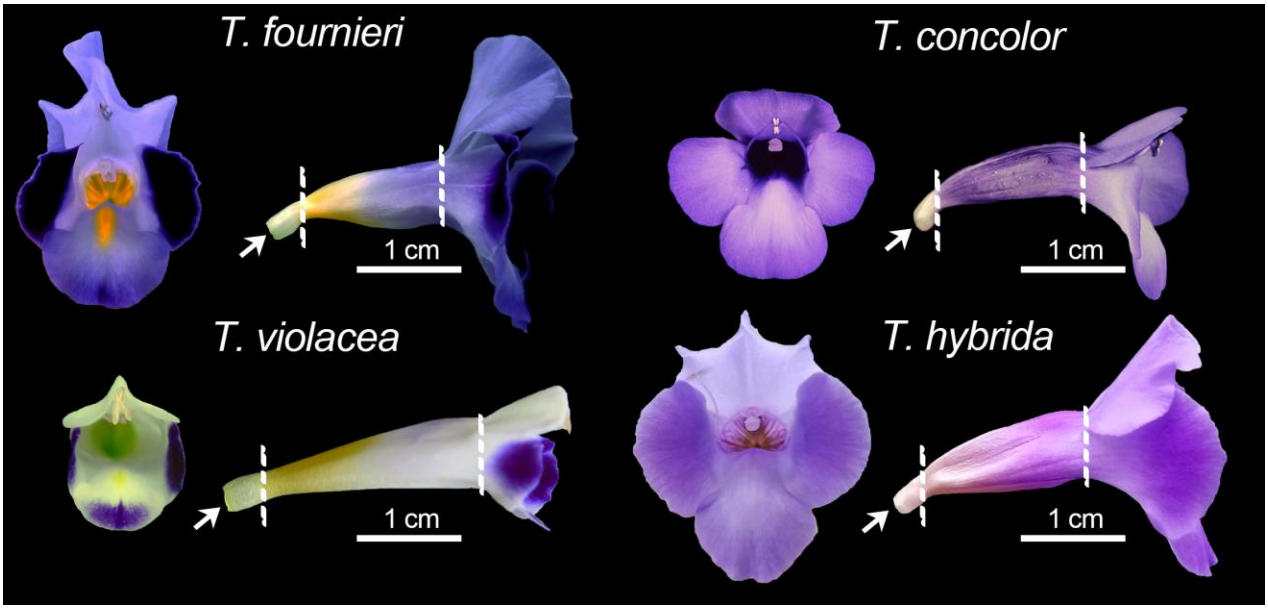

Fig. S1. Corolla morphologies of four *Torenia* species. Front and side views of each flower are shown. The dotted lines separate three different regions of the corolla, and the white arrows indicate the corolla neck.

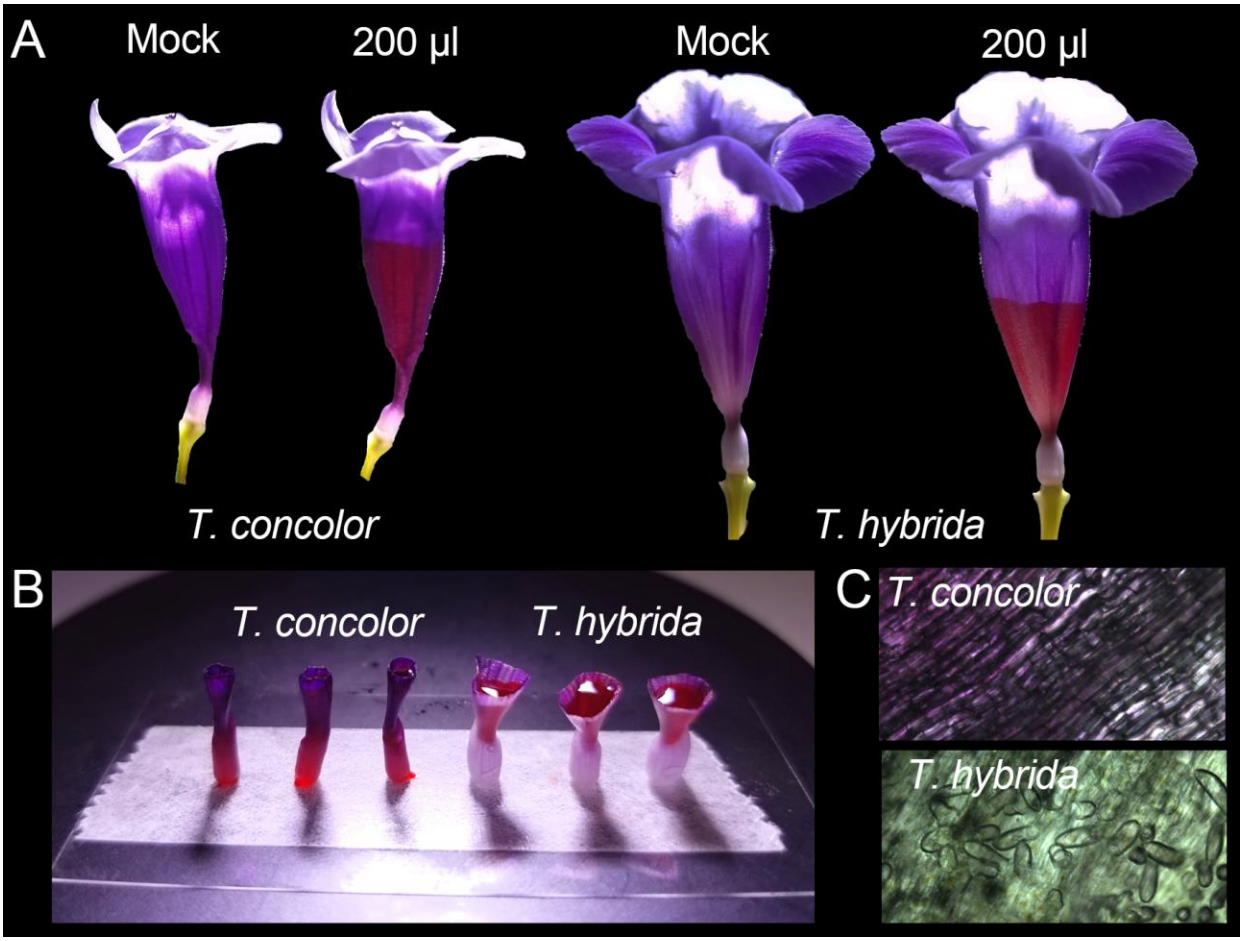

Fig. S2. Function and epidermal morphology of the corolla neck in *Torenia concolor* and *Torenia hybrida*. (A) Application of 200 µl water containing 0.1% Safranin O to a mature flower. (B) Application of 20 µl water containing 0.1% Safranin O to cut corolla bottoms. (C) Epidermal morphology of the corolla neck in *T. concolor* and *T. hybrida*.

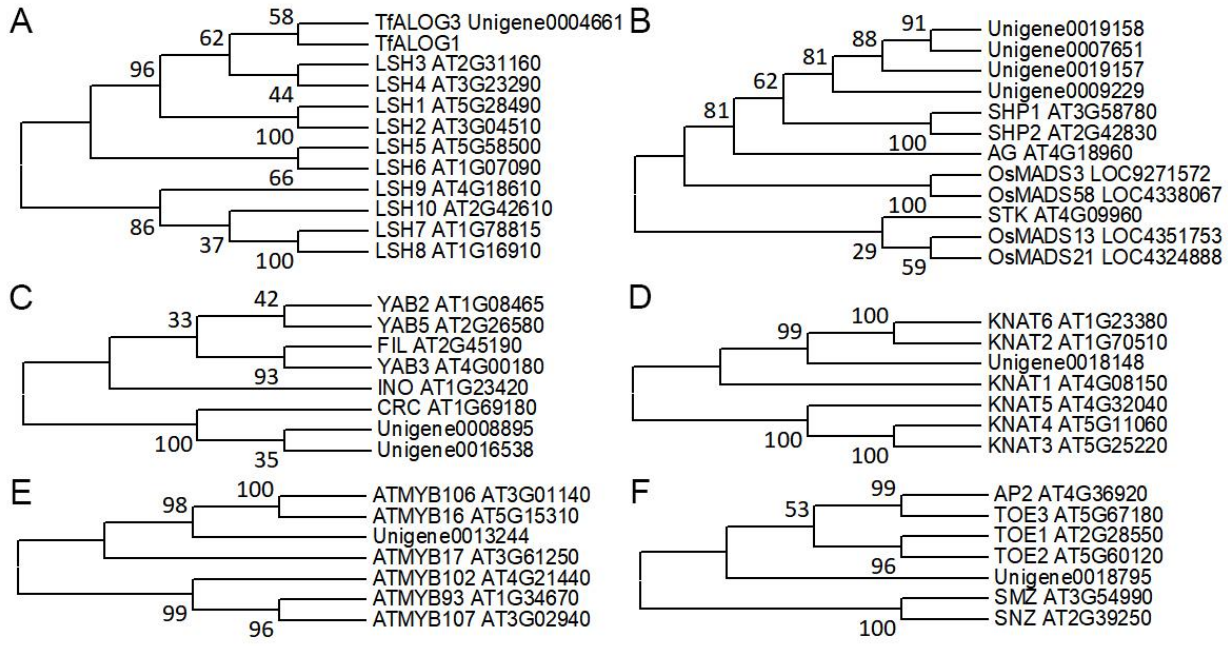

Fig. S3. Neighbor-joining trees for the top 10 enriched transcription factors. (A–F) The phylogenies of ALOG (A), MADS (B), YABBY (C), KNOX (D), MYB (E), and AP2 (F). The bootstrap value (percentage, based on 1000) is marked at each node, and the accession numbers are indicated as the suffix of each sequence.

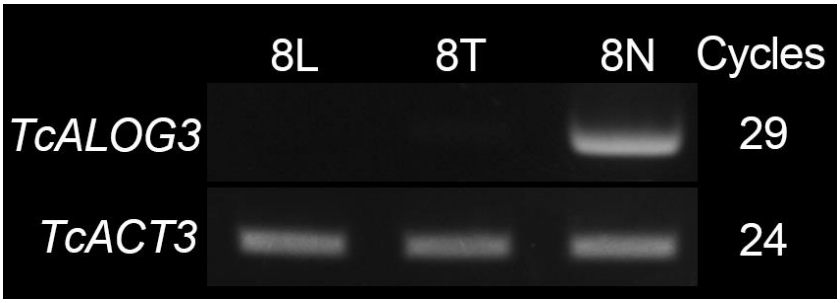

Fig. S4. Reverse-transcription PCR analysis in *Torenia concolor*. Gene names and number of PCR cycles are shown on the left and right sides of each panel, respectively. β-actin (*TcACT3*) expression was measured as an internal control. 8, 8 mm floral bud; L, petal lobe; T, conical petal tube; N, corolla neck.

A >TfALOG3 genomic DNA

ATGGACCCATCATTGTTCCCCAATCCTCAAAACGAGCCCACAAGCTCCGAGACCACCGCCAAC
ACCTACTCTGCAGCGACATCGTCGTCCTCCTCCACCTCCACCACCACCACCGCCGGCACATCCT
CCTCTTCCCGGTACGAGAACCAGAAACGCCGCGACTGGAACACCTTCAATCAGTATCTCAAGA
ACCACCGCCCGCCTCTCTCCCTCCACCGCTGCAGCGGGGCCCACGTCCTCGAATTTCTAAGGT
AGTAAGTAGTACTGCACCACTTGAACAAGAAACCTTTAAGTTTAATTGTTAAGACAGGGTGAG
TCGTGAGCAAGAATATGATCAAAGCGTTGAACGCGTTACTGTCGATAACAACTGATGTTGTAA
CGCAAACAAGTACGAGCAAAAGCTACACTGATAATATCTTATAACTCATAATTGGCCATCACAA
CATATCCCTAATTTACCTTATTTAATAAACGGCTGAGTTTCTCCCTCAATTCGGAGCTATTATTTT
CATCACGTTGTTGTTTTCGAGACTATCTTACTGCTGAACTACAGTTATTACATACGTGTTTGTTT
GTGTGTGTGTATATGTATGTATATATCTACCTCGCTATATCGTATAAACAGGTACCTTGACCAGTT
CGGCAAGACCAAAGTCCACAGCCCGGTCTGCCCGTTCTACGGAAACCCTAGCCCGCCTGCCC
CATGTCCCTGCCCGCTCCGACAGGCTTGGGGGAGCCTCGACGCGCTCGTCGGAAGGCTAAG
GGCAGCGTTCGAAGAGAATGGAGGAAAACCAGAGATGAACCCTTTCGGTGCAAGAGCCGTC
AGGCTCTATTTACGAGAAGTTCGTGACGTGCAGAGCAAGGCTCGAGGCGTCAGCTACGAGA
AGAAGAAGAGGAAGCGCCCGGCGGCAGCGGCTCAAGGCGGCGCGGCGGGTGACGAGGG
CAGCGATCAGCAGCCGGATACGTCTCCAAGTGAAGGGTAG

B

Yellow target 1 Yellow target 2

WT: ——ACCTCCACCACCACCAC-CGCCGG——GACGTGCAGAGCAAGG-CTCGAGG——
3#: ——ACCTCCACCACCACCACACGCCGG——GACGTGCAGAGCAAGGACTCGAGG——
19#: ——ACCTCCACCACCACCACACGCCGG——GACGTGCAGAGCAAGG-CTCGAGG——

Gray target 1 Gray target 2

WT: ——CCCATCA-TTGTTCCCCAATCCTC——CCAACACCTACTCTGCAGCGACA——
40#: ——CCCATCAATTGTTCCCCAATCCTC——CCAACACCTACTCTGCAGCGACG——

Gray target 3

WT: ——CAAGACCAAAGTCCACA-GCCCGG——
40#: ——CAAGACCAAAGTCCACAAGCCCGG——

Fig. S5. CRISPR/Cas9 genome editing. (A) The genomic DNA sequence of *TfALOG3*. The black and red characters represent exons and introns, respectively; PAMs (Protospacer Adjacent Motifs) are highlighted in green. Two CRISPR/Cas9 plasmids were used in this study, and the different CRISPR/Cas9 targets are highlighted in yellow and gray, respectively. Start and stop codons are highlighted in red. (B) Mutations in the WT and three *TfALOG3*-Cas9 plants.

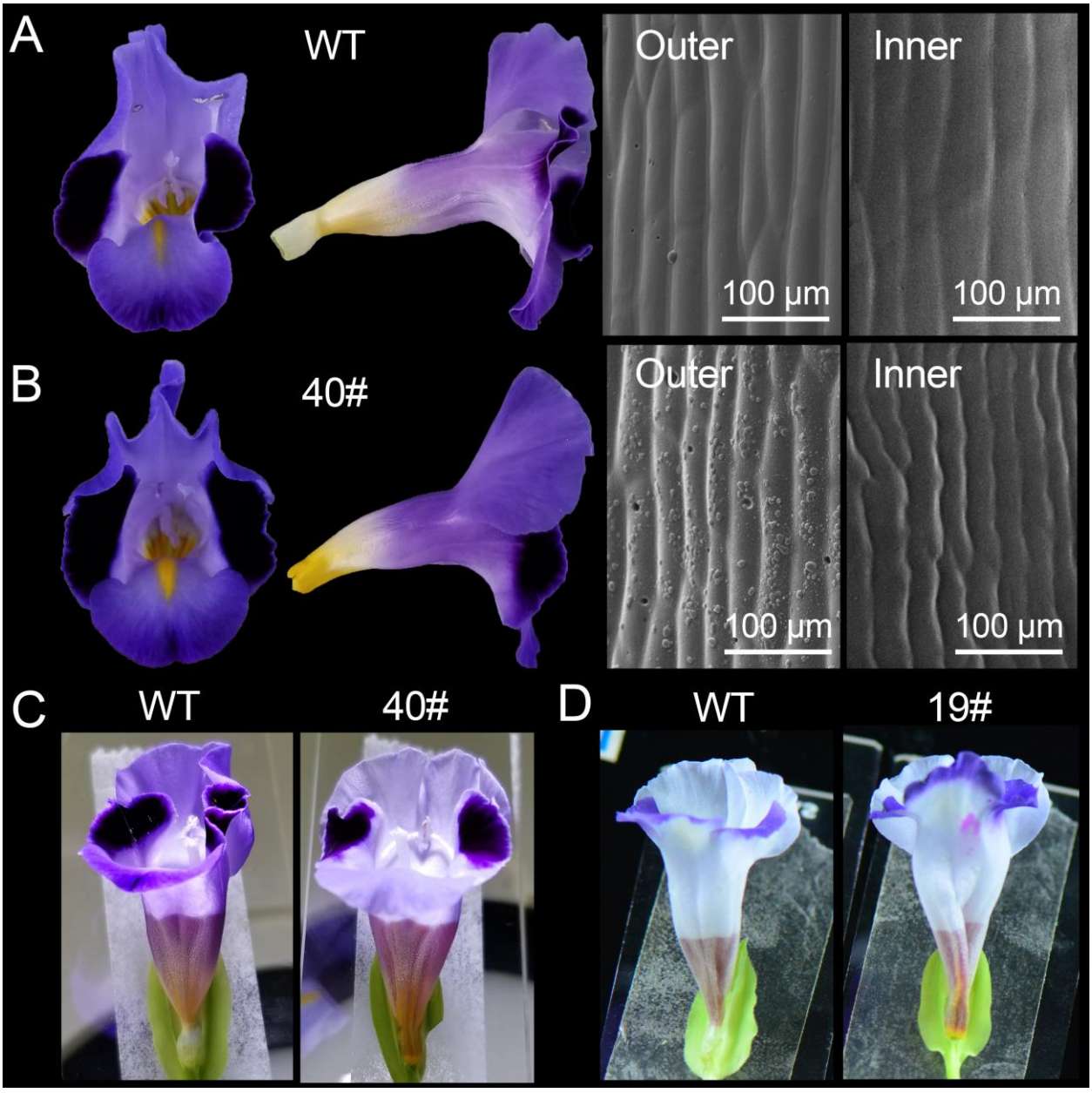

Fig. S6. Function and epidermal morphology of the corolla neck in the 19# and 40# transgenic lines. (A, B) Front and side views of *Torenia fournieri* wild-type (A) and *TfALOG3*-Cas9 40# (B) flowers. The outer and inner epidermal cell morphologies are also shown. (C, D) Application of 200 μl water containing 0.1% Safranin O to different flowers.

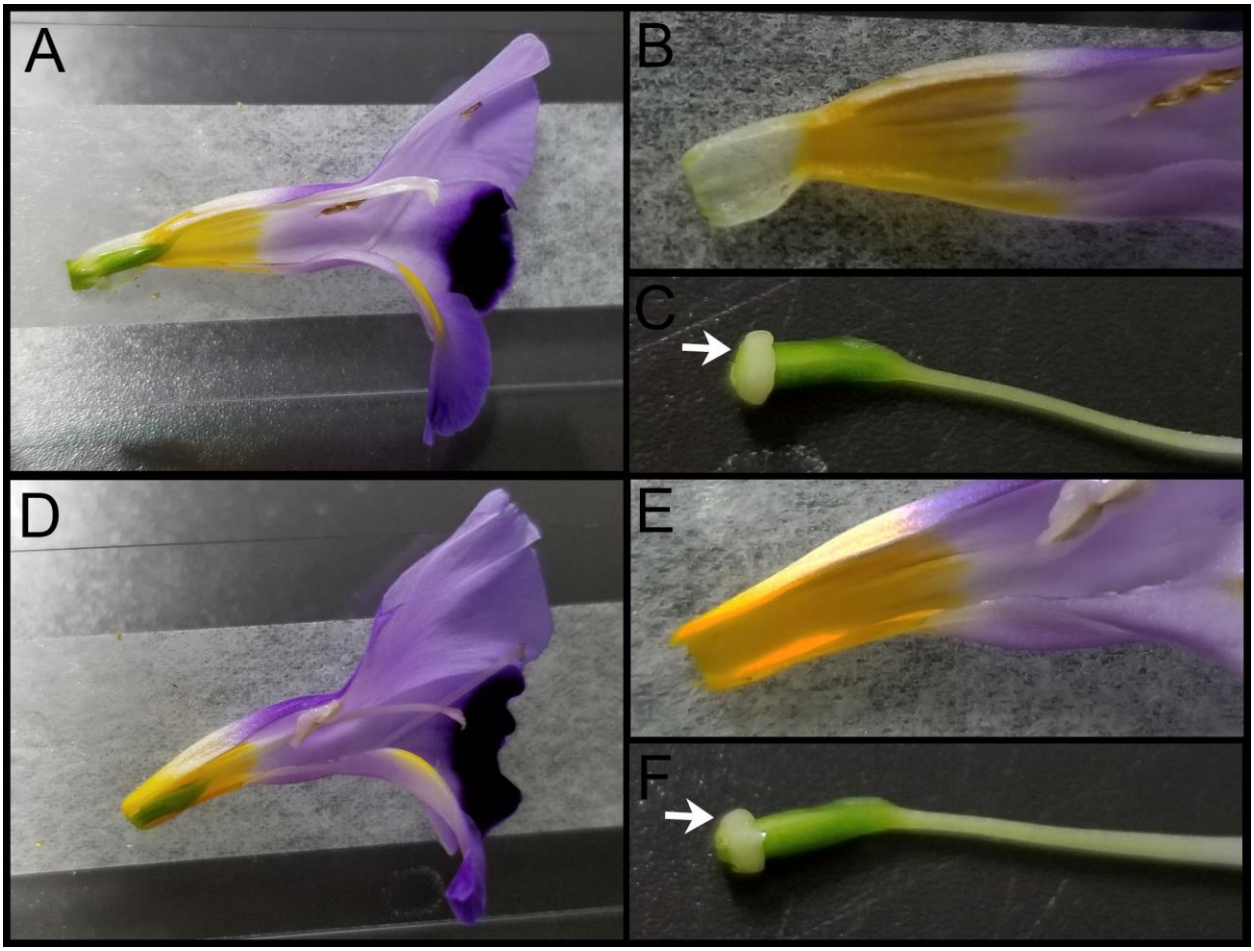

Fig. S7. Longitudinally dissected flowers from the WT and mutant plants. (A–F) Dissected WT (A–C) and 40# mutant (D–F) flowers. White arrows indicate the nectary in the floral base surrounding the ovary.

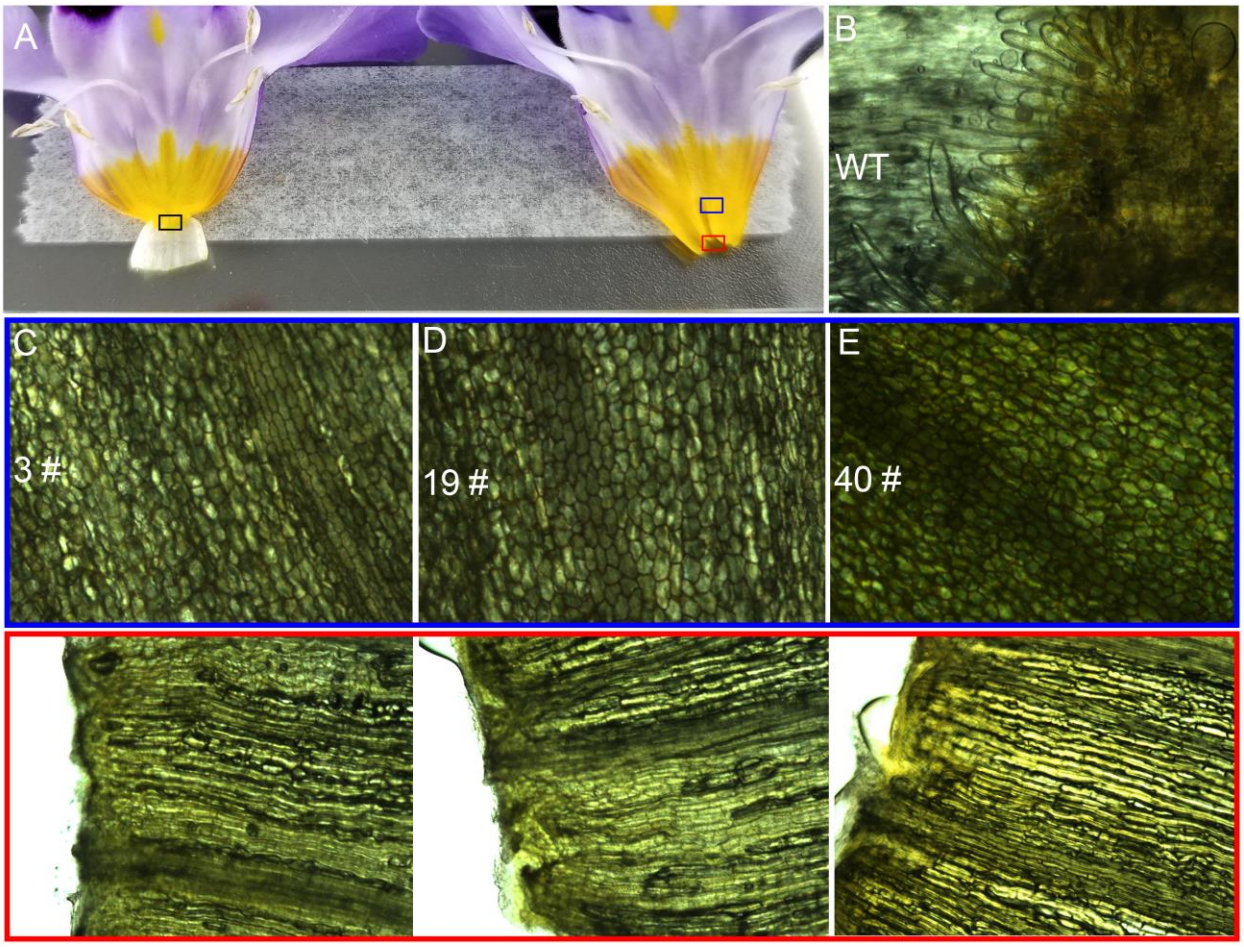

Fig. S8. Inner epidermis of the WT and mutant corolla bottoms. (A) Open corolla tubes from the WT (left) and mutant (right) plants. Black box indicates the regions being imaged in (B); blue and red boxes indicates the regions being imaged in (C-E). (B–E) Images of the WT corolla neck (B) and mutant corolla bottom (C–E).

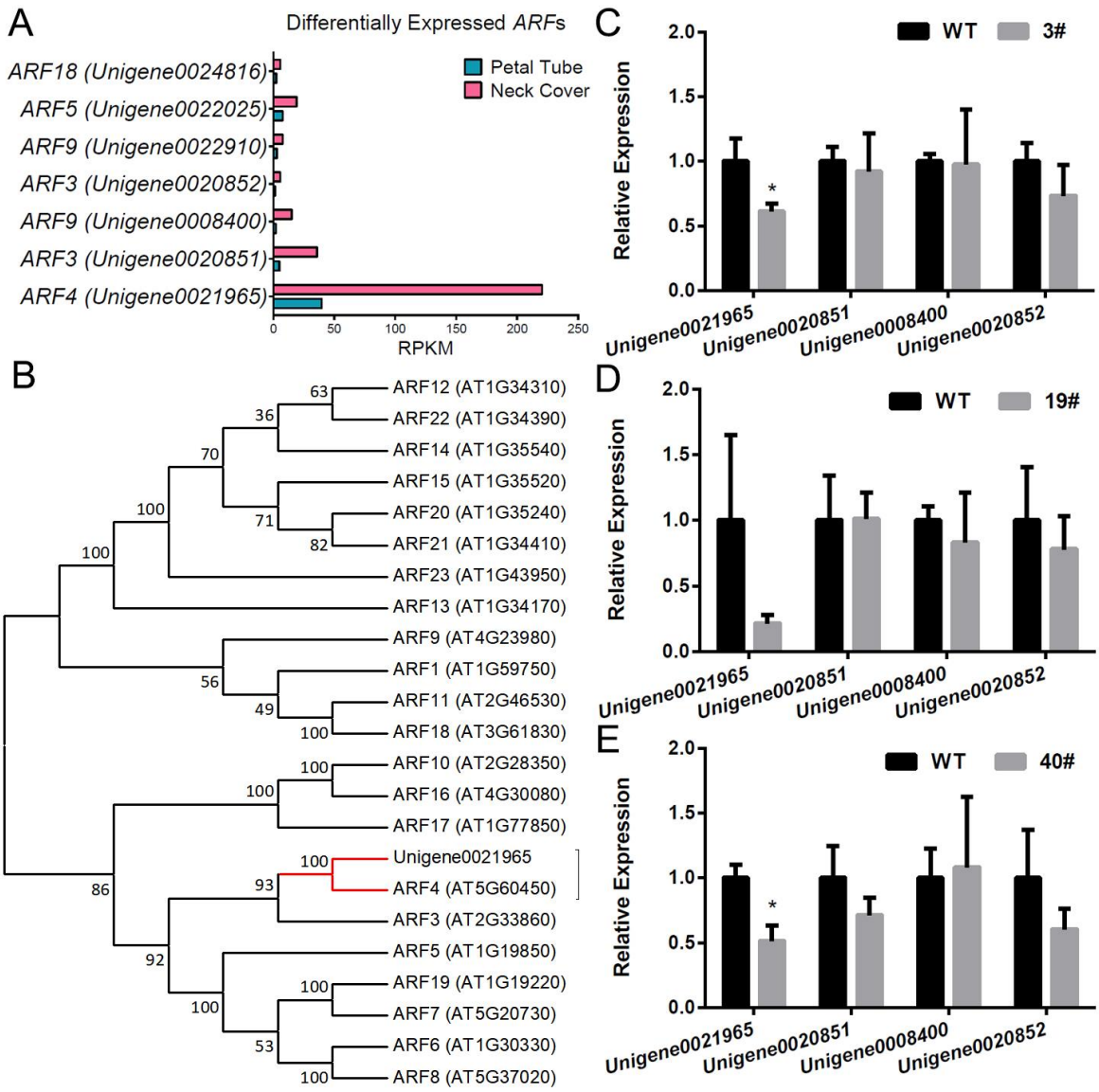

Fig. S9. Expression of *AUXIN RESPONSE FACTOR* (*ARF*) genes and a phylogenetic tree for ARF4. (A) Seven *AUXIN RESPONSE FACTOR*s enriched in the corolla neck according to transcriptomic analyses. The reads per kilobase per million mapped reads value for each unigene are shown. (B) A neighbor-joining tree for ARF4 together with all Arabidopsis ARF proteins. The red branch shows the relationship between Unigene0021965 and ARF4. The bootstrap value (percentage, based on 1000) is marked at each node, and the accession numbers are indicated as the suffix of each sequence. (C–E). Real-time PCR analysis of four *ARF* genes enriched in the corolla neck of the WT and three transgenic lines. The error bars are ± 1 SD from three biological replicates; asterisks indicate significant differences between the mutant and WT plants ($P < 0.05$).

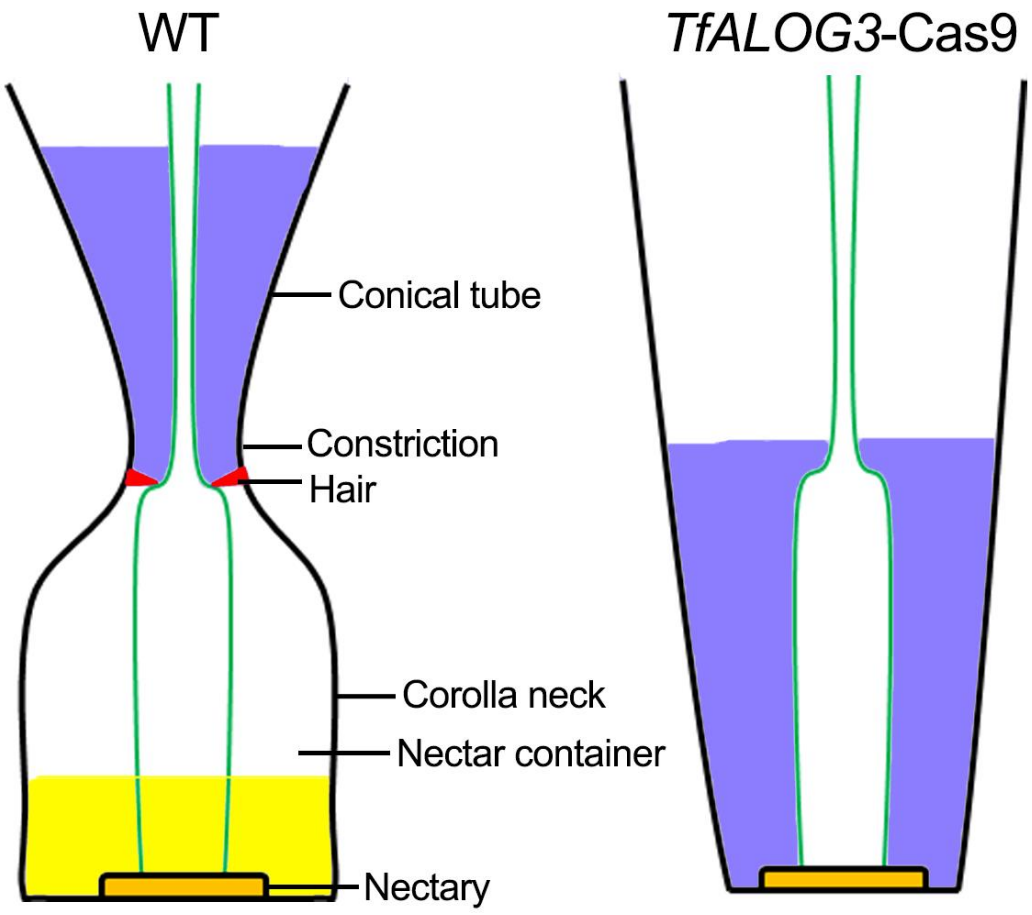

Fig. S10. Model of how the corolla neck prevents water from reaching the nectar container. The corolla, pistil, and nectary are shown in both the WT and mutant plants. Hairs in the constriction at the top of the corolla neck in WT plants are shown as red triangles; the blue block represents external water and yellow block the undiluted nectar.

Table S1. Primers used in this study.

Click here to Download Table S1

Table S2. Reads numbers, RPKM, FDR and annotation of differentially expressed genes.

Click here to Download Table S2